Journal of Engineering Physics and Thermophysics, Vol. 76, No. 5, 2003

CALCULATION OF OSCILLATIONS OF A CYLINDRICAL PENDULUM IN A CAVITY FILLED WITH A VISCOUS FLUID WITH THE USE OF SLIDING MULTIBLOCK GRIDS

P. A. Baranov, S. A. Isaev,
N. A. Kudryavtsev, and V. B. Kharchenko

UDC 532.517.2

The characteristics of the oscillations of a cylindrical pendulum in a square cavity filled with an incompressible viscous fluid have been forecast on the basis of the joint numerical modeling of two-dimensional unsteady laminar flow around a circular cylinder with the use of movable sliding grids and solution of dynamic equations.

Introduction. As is known, one of the classical problems of mechanics [1], concerning the interpretation of pendular oscillations, represents a conjugate problem in the case of a viscous medium, a correct solution of which reduces to the solution of the interrelated problems of the dynamics of a moving body and numerical modeling of unsteady flow of a viscous fluid around it. However, this conjugate problem has not yet been considered in such a formulation. Progress in computational methods in hydromechanics has made it possible to solve it in a simplified two-dimensional representation, which has been done in the present work.

It is interesting to consider the genesis of the proposed computational algorithm, which is based on the multiblock computational technologies developed. The impetus to such developments has been given by the numerical investigations of separated flow around bodies of multiply connected different-scale arrangements, such as a thick profile with vortex cells [2]. The characteristic features of the computational procedure based on the use of intersecting structurized grids were described for the first time in [3] by the example of numerical modeling of laminar flow around a cylinder with a circular cavity built into its contour with a central body positioned in the cavity. One of these features is the multistage structure (with a different density of cells, depending on the distance from the wall) of the computational grids near a body around which flow flows, which allows one to distinguish different-scale elements of the flow, such as the boundary layer and separation zones, with a high degree of accuracy. Hereinafter, the multistage grids make it possible to pass to the use of low-Reynolds models of turbulence, in particular, Menter's zonal model of shear-stress transfer [4].

The multiblock approach to solution of nonstationary problems of hydromechanics has been tested and verified in calculating a two-dimensional flow around a circular cylinder and around bodies with vortex cells [5–9]. Detailed consideration has been given to modeling of the vortex dynamics at the instant a circular cylinder begins to move, in the autooscillation regime of flow around a circular cylinder with a Kármán vortex street, in the case where artificial vorticity is generated by active vortex cells in the near wake behind a cylinder and an elongated body, and in the case where a cylinder is surrounded by a housing with windows which enable the fluid to flow from the region of high pressure to the regions of low pressure with the formation of fairly intense jets.

The multiblock approach developed has been extended to the problems of steady three-dimensional laminar and turbulent flows around objects of various geometry, in particular, around a set of spherical holes on the wall of a narrow channel [10]. In [11], a comparative analysis of the results of numerical and physical modeling of a low-velocity air flow in a rectangular channel with a circular cavity on one of the walls has been performed.

In the present work, the multiblock computational technologies have been extended to the case of self-propelled bodies. In contrast to [12], where the forced transverse oscillations of a plane rectangular body in a turbulent flow have been calculated using a system of initial equations containing an additional source term introduced because

Academy of Civil Aviation, St. Petersburg, Russia; email: isaev@SI3612.spb.edu. Translated from Inzhenerno-Fizicheskii Zhurnal, Vol. 76, No. 5, pp. 61–70, September–October, 2003. Original article submitted December 19, 2002.

1062-0125/03/7605-1024$25.00 ©2003 Plenum Publishing Corporation

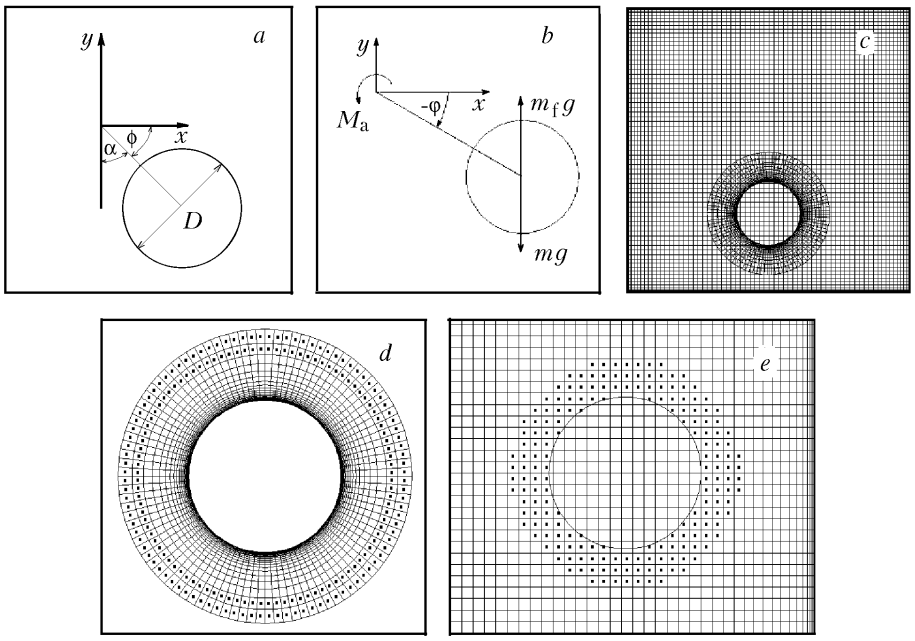

Fig. 1. Scheme of the computational region with a circular cylinder executing oscillatory motions (a), designations for calculation of pendular oscillations (b), and multiblock computational grids (c) with connected cells on the sliding (d) and immovable (e) grids.

of the use of the noninertial coordinate system, here we realize an approach analogous to that in [13]. In accordance with this approach, a body surrounded by a grid consistent with its contour moves in a selected region in which a flow of the medium surrounding the body is described on an immovable computational grid.

Formulation of the Problem. A conjugate problem on oscillatory motion of a pendulum, as which a circular cylinder is used, and unsteady laminar flow of a viscous fluid in a square cavity (Fig. 1a) is solved. The point of suspension of the pendulum is positioned at the center of the region. The origin of the Cartesian coordinate system *x*, *y* is brought into coincidence with this point.

Equation of pendulum motion. We introduce the Cartesian coordinate system as is shown in Fig. 1b. Let the gravity force be directed downward.

The dimensional equation of rotation about the *z* axis has the form

$$J\frac{d\omega}{dt} = M_a + (m_f - m)\, gR\cos\varphi\,. \tag{1}$$

We introduce the characteristic linear dimension *L*, characteristic area *S*, and characteristic velocity *V*. Then

$$\omega = \bar{\omega}\frac{V}{L},\quad t = \bar{t}\frac{L}{V},\quad J = \int_\Omega \rho_b r^2 d\Omega = \rho_b L^5 \int_\Omega \bar{r}^2\, d\bar{\Omega} = \bar{J}\rho_b L^5;$$

$$m = \int_\Omega \rho_b d\Omega = \rho_b L^3 \bar{\Omega},\quad m_f = \int_\Omega \rho_f d\Omega = \rho_f L^3 \bar{\Omega};$$

$$M_a = m_a SL\frac{\rho_f V^2}{2} = m_a \bar{S}L^3\frac{\rho_f V^2}{2}.$$

Substituting these expressions into (1), we obtain

$$\bar{J}\rho_b L^3 V^2 \frac{d\bar{\omega}}{d\bar{t}} = m_a \bar{S} L^3 \frac{\rho_f V^2}{2} + \bar{\Omega} L^4 (\rho_f - \rho_b) g\bar{R} \cos\varphi$$

or

$$\bar{J} \frac{d\bar{\omega}}{d\bar{t}} = m_a \frac{1}{2} \bar{S} \frac{\rho_f}{\rho_b} + \bar{\Omega} \frac{Lg}{V^2} \left(\frac{\rho_f}{\rho_b} - 1 \right) \bar{R} \cos\varphi .$$

Let us introduce the notations

$$\mathrm{Nt} = \frac{\rho_f}{\rho_b}, \quad \mathrm{Fr} = V/\sqrt{gL} .$$

In the final analysis we obtain

$$\bar{J} \frac{d\bar{\omega}}{d\bar{t}} = m_a \frac{1}{2} \bar{S}\, \mathrm{Nt} + \bar{\Omega}\, \mathrm{Fr}^{-2} (\mathrm{Nt} - 1)\, \bar{R} \cos\varphi . \tag{2}$$

In the program, in calculating the moment, the forces are simply integrated over the surface without referring to any area, and the pressure refers to ρV^2 and not to $\rho V^2/2$. This corresponds to some other nondimensional representation of the moment, namely, $M_a = \bar{M}_a L^3 \rho V^2$. In this case, the equation of motion will take the form

$$\bar{J} \frac{d\bar{\omega}}{d\bar{t}} = \bar{M}_a\, \mathrm{Nt} + \bar{\Omega}\, \mathrm{Fr}^{-2} (\mathrm{Nt} - 1)\, \bar{R} \cos\varphi . \tag{3}$$

The maximum rate of the pendulum motion without regard for the influence of the hydrodynamic forces U and the diameter of the cylinder D are taken as the dimensionless scales.

The problem on unsteady two-dimensional laminar flow of an incompressible viscous fluid around a circular cylinder is solved using a mathematical model based on the system of Navier–Stokes equations.

Computing method. The computational multiblock algorithm [7–9] is based on the procedure of global iterations, which has been developed for solving transfer equations by the finite-volume method on intersecting structurized H- and O-type grids (Fig. 1c). The most applicable approach to description of flows in the generalized curvilinear coordinates is the use of grids with a centered template where all the dependent variables are prescribed at the centers of the cells [14].

In the multiblock methodology developed, the grid cells are subdivided into computational and connected cells.

The computational cells are cells in which the initial equations are solved. The latter are written in the delta form in curvilinear coordinates, consistent with the boundaries of the computational region, relative to the increments of dependent variables, including the Cartesian velocity components. After linearization, the system of initial equations is solved using the SIMPLEC-type finite-difference procedure of pressure correction [14], which is based on the concept of splitting by physical processes and is written in the *E*-factor representation. The upwind scheme with quadratic interpolation is used in the explicit side of the transfer equations to decrease the influence of numerical diffusion in calculations of flows with organized flow separation, which are very sensitive to the errors in the approximation of the convective terms [14]. At the same time, to avoid false oscillations in the reproduction of flows with thin shear layers, the mechanism of artificial diffusion is used in the implicit side of the equations in combination with unilateral upwind schemes for representation of convective terms. And, to eliminate the nonmonotonicity of the pressure field in the discretization of the pressure gradient by the central-difference scheme on the centered template, a monotonizer [14] with an empirical cofactor, determined in the numerical experiments on flow of an incompressible viscous fluid around a cylinder and a sphere and equal to 0.1, is introduced into the block of pressure correction. High efficiency of the computational procedure for solving discrete algebraic equations is insured by the use of the method of incomplete matrix factorization [14]. By and large, the methodology developed is fairly original and differs from the analogs [15].

The connected cells are cells in which the values of the parameters are determined by interpolation of data from other regions. Numerous test calculations (see, e.g., [4–9]) have shown that the nonconservative linear interpolation is wholly acceptable.

In all the connected cells, the source terms are assumed to be zero and the coefficients of the unknowns in the algebraic equations, except for a_p equal to unity [14], are also zero. Therefore, the calculation is performed by the through method over the whole region. An additional memory for storage of the metric and variables is provided for the bounds of the computational cells, coincident with the outer boundary of the region or with the boundary of the body. At all the other bounds the values are determined in the ordinary way by interpolation. A computational cell must have at least two neighbors on the side of these bounds to provide the second order of approximation of the convective terms.

The connected cells can be conditionally subdivided into two groups — the cells that are compulsorily specified to be connected (they are, as a rule, the peripheral layers of internal grids) and the cells specified to be connected in the process of generation of grids. This division is merely a convention that is determined only by the method of specification. Otherwise these cells are identical.

Figure 1d shows the connected cells of the periphery of the pendulum grid. They are specified from the outset. However, prior to calculating, the cells of the external grid, which are entirely positioned within the pendulum grid, must be specified to be connected cells (Fig. 1e). If this is not done, the external grid will "know" nothing about the existence of the pendulum. Clearly, for this problem, they are specified over again at each time step.

Prior to solving each equation, the variables in the connected cells are calculated. This does not take much time because the interpolation coefficients are determined in advance. Then one iteration step is made in each region. It makes no difference in which order the regions are scanned. The corrections to a given variable are determined when passing to the next iteration (not global but for the selected equation). This is of no significance for the equation of velocity transfer since only one iteration is made as a rule; for the majority of other variables, the absence of this step somewhat decelerates the convergence, but practically imperceptibly. And only for the pressure is consideration of corrections taken from other regions of fundamental importance because this is a single mechanism that makes it possible to automatically find the constant within which the pressure is determined.

The algorithm proposed allows one to easily construct the procedure of calculation of flow on sliding grids like the grids presented in Fig. 1c.

Computational grids. The circular pendulum is surrounded by a cylindrical grid containing 30×100 cells arranged with bunching to the pendulum surface. It is assumed that the grid pitch along the peripheral coordinate is constant and the near-wall radial pitch is equal to 10^{-4}. The region around the pendulum extends to 0.5. The length of the inflexible and imponderable connection connecting the point of suspension and the center of mass of the pendulum executing oscillatory motions is equal to unity.

The square cavity filled with a viscous fluid, in which the cylindrical pendulum swings, has dimensions 4.5×4.5. The distribution of the grid points along the horizontal and the vertical of the cavity is the same. Twenty cells are positioned at a distance of 0.75 from the wall with a near-wall pitch of 10^{-3}. Twenty cells are positioned with an approximately equal pitch of 0.07 in the next region from the wall to the center of the cavity of dimension 1.5.

Initial and boundary conditions. The initial position of the cylindrical pendulum is horizontal, i.e., $\varphi = 0^o$ or $\alpha = 90^o$. At each point of the pendulum surface around which fluid flows, the Cartesian velocity components of the flow are prescribed to be equal to the corresponding components of the velocity of travel of the selected point in the process of pendulum motion. Ordinary adhesion conditions are set on the surface of the cavity. Fluid flow is absent at the initial instant of time and the initial angular, rotational velocity of the cylinder is equal to zero.

Results of calculations. The problem on oscillations of a cylindrical pendulum is solved at the Reynolds number Re = 100 and the Froude number Fr = 1. The ratio between the densities of the fluid and the pendulum is taken to be 0.37.

The set of prescribed parameters corresponds to the following physical conditions: an aluminum pendulum of density 2670 kg/m^3 and diameter 0.125 m is positioned in a square cavity filled with an oil of density 903 kg/m^3 at a temperature of 20^{o}C (the kinematic viscosity coefficient is equal to $1.547 \cdot 10^{-3}$). Under these conditions, the maximum rate of pendulum motion is 1.2 m/sec and the period of its oscillations is equal to 1.092 sec without regard for

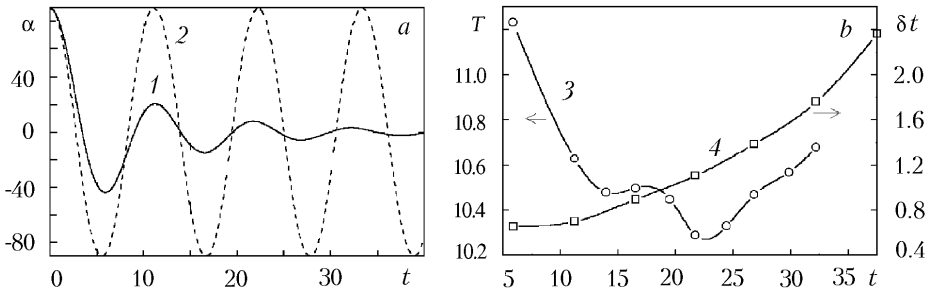

Fig. 2. Comparison of the time dependences of the (a) angular deflections of the pendulum in the viscous (1) and nonviscous (2) fluid and (b) oscillation period (3) and the time intervals within which the pendulum stays at the extreme positions (4).

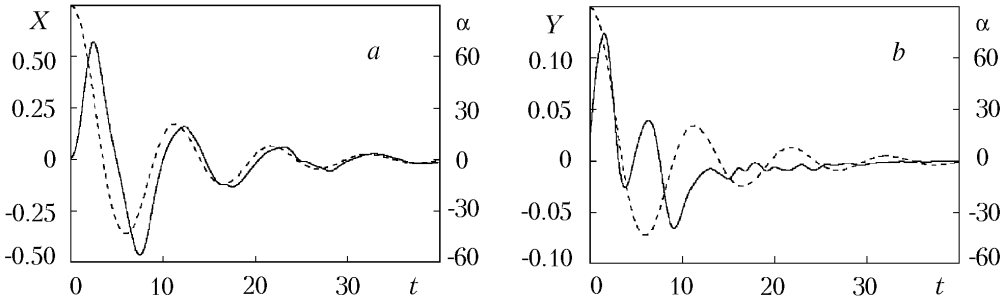

Fig. 3. Time dependence of the horizontal (a) and vertical (b) components of the drag force; the dashed curves are the time dependences of the angular deflections of the pendulum.

the influence of the viscous medium. Then the set of controlling parameters of the problem is as follows: Re = 99.2, Fr = 0.85, and Nt = 0.338, i.e., they are very close to the prescribed ones.

Thus, we consider the problem on oscillations of the aluminum pendulam in the oil with allowance for the walls bounding the cavity. In solving this problem, the ordinary differential equation (3) is integrated with a selected step Δt equal to 0.01 by the Runge–Kutta method. The velocities of travel of the center of mass and of the points of the cylinder contour, which are used as the boundary conditions for calculating a flow around the cylinder, are determined at each time step. The system of nonstationary Navier–Stokes equations for an incompressible viscous fluid is solved using the methodology described in detail in [7–9] to calculate the local and integral force loads on the cylinder and the torque moment M_a. The time step used in modeling of flow around the cylinder is taken to be equal to the step of integration of the dynamic equation. At each time step, the aerodynamic moment is determined using the relaxation procedure with the coefficient 0.25 (selected from the calculations by the method of discrete vortices [16] to ensure the monotony of the solution on the basis of smoothing of oscillations).

Figures 2–9 show some of the calculation results obtained.

As follows from Fig. 2a, the pendular oscillations in the viscous medium at Re = 10^2 are damped in character. At the prescribed parameters, the maximum angle of deflection of the pendulum from the vertical decreases approximately by one-half in the process of successive deflections of it to the right and to the left. To the instant t = 40, the amplitude α enters the range 2^o. In this case, if at the beginning of the process the pendular oscillations differ strongly from the isochronous oscillations [1], after the first period they become qualitatively similar to the isochronous oscillations of a pendulum in a nonviscous medium of the same density (with allowance for the buoyancy force). Judging from Fig. 2b, the oscillation period represents a function that decreases with time in the two first oscillation periods and then monotonically increases in the limiting range of change. The functional dependence of the time interval within which $|\alpha - \alpha_{ext}| < 0.5^o$ is close to the square law in character. This means that the time of stay of the pendulum at its extreme positions increases with increase in t.

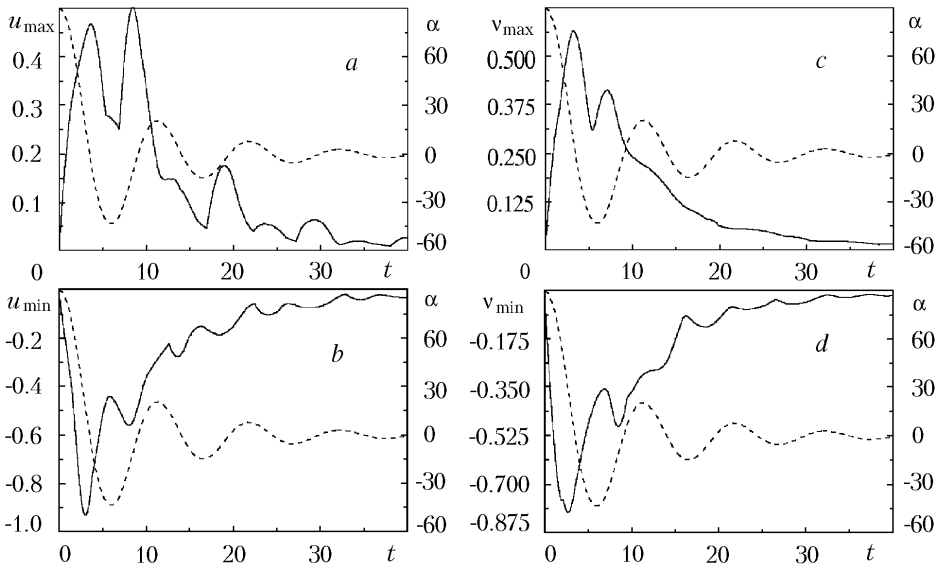

Fig. 4. Time dependences of the maximum (a, c) and minimum (b, d) values of the horizontal (a, b) and vertical (c, d) velocity components; the dashed curves are the time dependences of the angular deflections of the pendulum.

The further analysis concerns the correlations between the time changes in the integral force characteristics and in the extremum values of the local parameters of the flow and the evolution of the structure of the flow around the cylinder executing oscillatory motions.

As follows from Fig. 3a, by and large the damped oscillations of the horizontal, hydrodynamic drag force for the cylinder are harmonic in character and shifted in phase relative to the pendular oscillations. It is evident that this force is absent when the pendulum is at the initial extreme position where it is at rest. However, the indicated component of the drag force rapidly increases when the pendulum begins to move and the velocity of its travel increases; it reaches the maximum on the descending trajectory of the pendulum. The zero value of $X(t)$ corresponds to the near-extreme left position of the cylinder. It is reasonable that at the extreme left position, the horizontal component of the drag force is not maximum and continues to increase in absolute value for a certain time until the local minimum of $X(t)$ is realized. It is significant that the first local minimum of $X(t)$ differs in value only slightly from the first local maximum, whereas the oscillation amplitude $\alpha(t)$ decreases by half. Hereinafter, the situation recurs, i.e., the second maximum and the second minimum differ little from each other, etc. At $t > 15$ the oscillations of $X(t)$, especially of $Y(t)$, become nonharmonic.

The behavior of the vertical component of the drag force of the circular cylinder executing oscillatory motions is characterized by two dependences $Y(t)$ different in form (Fig. 3b). In the first period of the pendular oscillations (approximately to t = 14) the damped harmonic oscillations of $Y(t)$ change to oscillations of more complex form representing a superposition of harmonics. The reason for their appearance is the influence of the walls bounding the cavity or, more precisely, the surrounding-medium motion induced by the pendulum motion.

The extremum values of $Y(t)$ are more than four times smaller than the corresponding values of $X(t)$. During the half-period of pendular oscillations the vertical component of the drag force manages to execute the complete period of oscillations. When the pendulum goes from the descending to the ascending portion of its trajectory, $Y(t)$ changes sign as a natural result; then it gains not only the extremum negative value but also the maximum positive value at the near-extreme left position of the pendulum. It should be noted that at the end of the first period of pendular oscillations the vertical component of the drag force does not change sign, i.e., it remains negative.

In the second and subsequent periods of pendular oscillations, $Y(t)$ continues to be negative despite the local oscillations caused by the influence of the walls bounding the cavity.

It is very interesting to investigate the regularities of the time behavior of the extremum parameters of the flow, presented in Fig. 4. It is obvious that the damping process of pendular oscillations correlates with the general regressive character of the change in the horizontal and vertical velocity components.

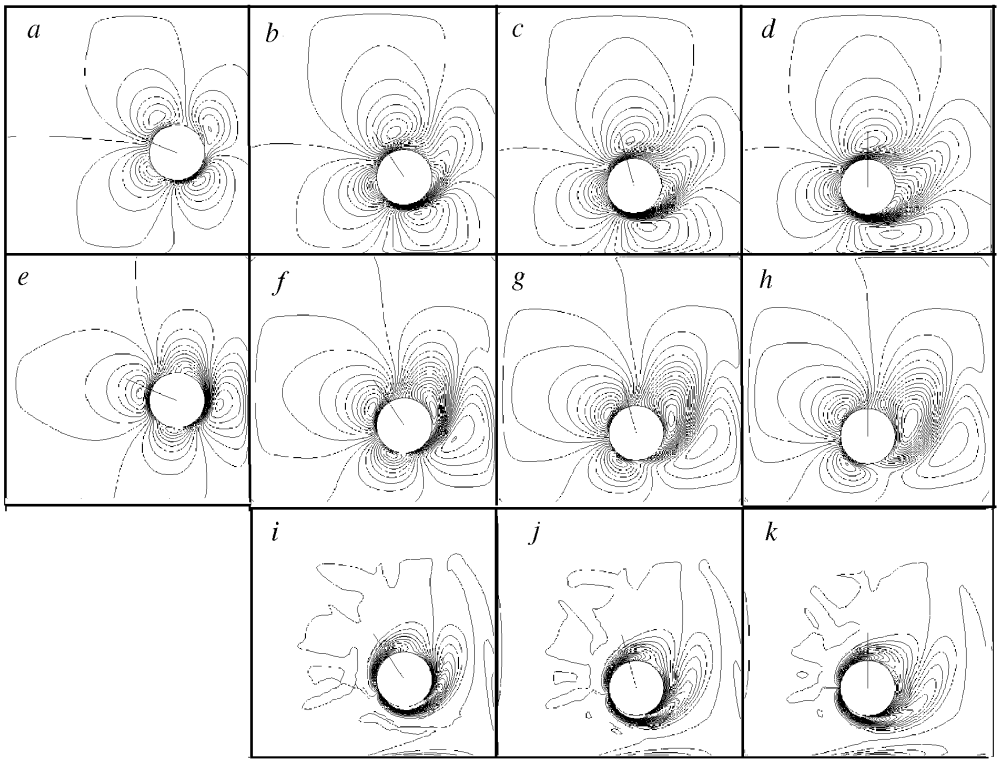

Fig. 5. Evolution of the patterns of flow around the circular cylinder in the first quarter of the first period of the pendular oscillations. The fields of isolines of the horizontal (a, b, c, d) and vertical (e, f, g, h) velocity components are drawn with a step of 0.05 and the fields of vorticity isolines (i, j, k) are drawn with a step of 0.5. The patterns were constructed at the instants of time t = 1.5 (a, e), 2.5 (b, f, i), 3 (c, g, j), and 3.45 (d, h, k).

The time dependence of the positive maximum value of the horizontal velocity component of the flow is divided into several characteristic portions (Fig. 4a). The first of them, corresponding to the rapid increase in $u_{max}(t)$ in the process of accelerated motion of the pendulum along the descending trajectory, is determined by the increasing velocity of its travel. The pendulum motion initiates a counterflow of the viscous fluid around the circular cylinder. The counterflow gathers the maximum velocity at the lower point of the trajectory (u_{max} is of the order of 50% of the characteristic velocity). Then the velocity of the flow around the body decreases by the harmonic law approximately to the level 0.28; the deflection of the dependence $u_{max}(t)$ corresponds to the near-extreme left position of the pendulum. The initial portion of the time dependence of the maximum horizontal velocity component, after its deflection, ends with a short descending convex segment corresponding to the time of stay of the cylinder at the extreme position. By and large, the initial portion is virtually coincident with the half-period of the pendular oscillations. It is significant that hereafter this portion will recur in form on the plot $u_{max}(t)$ and correspond to the descending portions of the curve $\alpha(t)$.

The second abrupt increase in $u_{max}(t)$ as a natural result is larger than the first one, because it is determined by the powerful carrying action of the pendulum. However, the increase in the local maximum is small (0.5). The next three abrupt increases in $u_{max}(t)$ in the process of oscillatory motion of the pendulum correspond to the ascending trajectory $\alpha(t)$ and have very different values (0.18, 0.07, and 0.025).

The behavior of $u_{min}(t)$ is analogously ordered (Fig. 4b). The first abrupt increase in the minimum value of the horizontal velocity component, which is due to the carrying action of the pendulum and is very equal in absolute value to the maximum characteristic velocity of the problem, is followed by several zigzag portions. Each of them includes a near-harmonic segment of the decreasing dependence $u_{min}(t)$ with three extremum values, which corresponds to the left position of the pendulum, and a segment differing from the harmonic with a knee corresponding to the right extreme position of the pendulum. It should be noted that the local extrema of $u_{min}(t)$ and $u_{max}(t)$ correlate with each other both in value and in position.

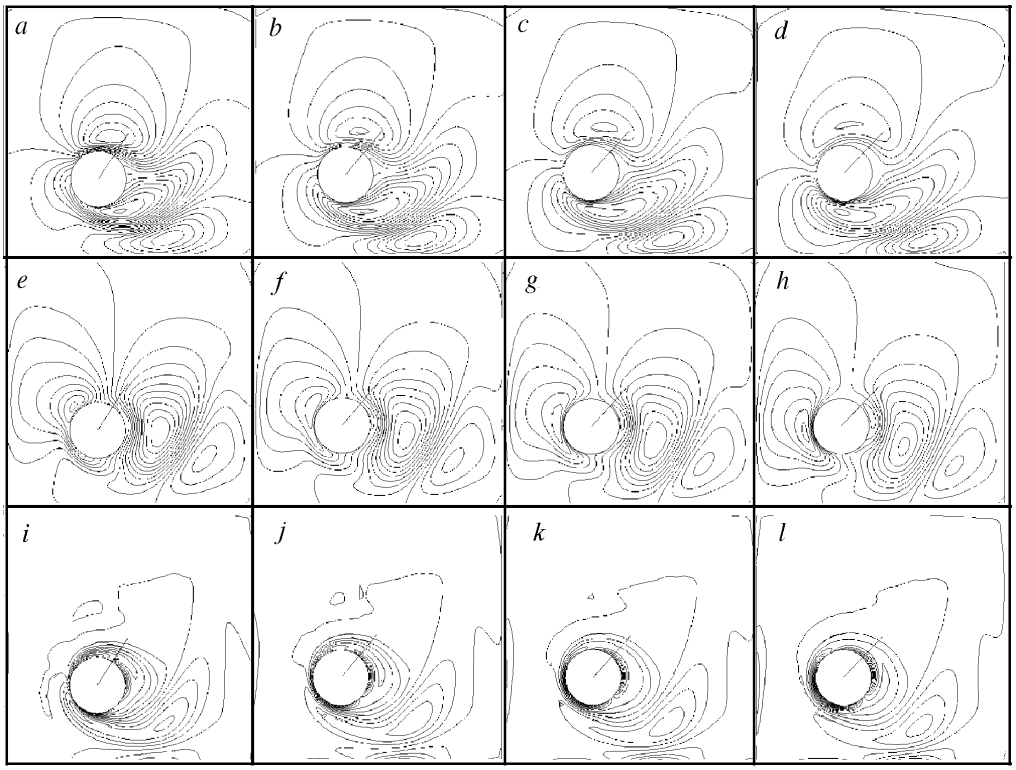

Fig. 6. Evolution of the patterns of flow around the circular cylinder in the second quarter of the first period of the pendular oscillations. The fields of isolines of the horizontal (a, b, c, d) and vertical (e, f, g, h) velocity components are drawn with a step of 0.05 and the fields of vorticity isolines (i, j, k, l) are drawn with a step of 0.5. The patterns were constructed at the instants of time t = 4.7 (a, e, i), 5.2 (b, f, j), 5.5 (c, g, k), and 5.9 (d, h, l).

Judging from Fig. 4c, the maximum (positive) vertical velocity component is less prone to oscillations. Only the initial phase of the pendulum motion causes a fairly strong counterflow of the viscous fluid (whose velocity reaches 55% of the maximum velocity). The local minimum of the vertical velocity component (0.32) corresponds to the ascending portion of $\alpha(t)$ and is determined by the carrying action of the body, and the second local maximum of $v_{max}(t)$ corresponds to the extreme left position of the pendulum. Hereinafter, a monotonous regressive dependence $v_{max}(t)$ is virtually realized.

The minimum (negative) vertical velocity component is more prone to time changes (Fig. 4d). The oscillations of $v_{min}(t)$ are more marked in the initial phase of the process even though the vertical velocity component, which is maximum in absolute value in the period of touch of the pendulum (approximately 80% of the maximum, characteristic velocity), is lower than the analogous horizontal velocity component (Fig. 4b). The dependence $v_{min}(t)$, as also $u_{min}(t)$, has a local minimum (in modulus) at the extreme left position of the body. Hereinafter, numerous local extrema of $v_{min}(t)$ are realized even though they are defined not so clearly as the extrema of $u_{min}(t)$.

The later patterns of unsteady laminar flow around the circular cylinder executing oscillatory motions, presented in Figs. 5–9, correspond to the first periods of the pendular oscillations and to the instants of time at which the integral force loads and the extremum local characteristics of the flow have maximum and minimum values.

The initial phase of the flow around the cylinder is realized on the descending trajectory of the pendulum (Fig. 5). Even at the first instants corresponding to the deflection of the cylinder from the horizontal position, oppositely directed flows arise near it. Before and behind the cylinder there arise zones of negative Cartesian velocity components, because of the piston effect, including discharges behind the cylinder (the largest values are approximately equal to 0.4–0.45 before and 0.6 behind the cylinder). Thus, the body carries the fluid after it and, at the same time, brings the fluid before it up to speed. In the central region of the cavity and in the near-wall zones adjacent to the

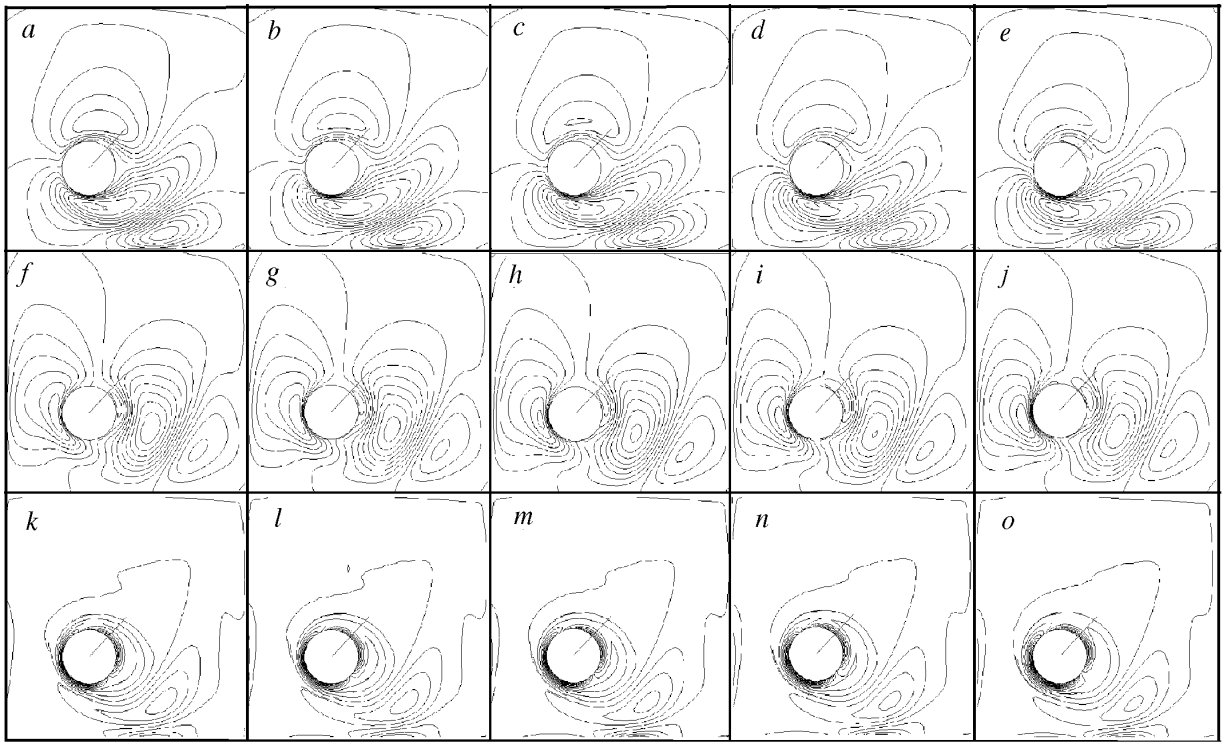

Fig. 7. Evolution of the patterns of flow around the circular cylinder at the near-extreme left position of the pendulum. The fields of isolines of the horizontal (a, b, c, d, e) and vertical (f, g, h, i, j) velocity components are drawn with a step of 0.05 and the fields of vorticity isolines (k, l, m, n, o) are drawn with a step of 0.5. The patterns were constructed at the instants of time t = 5.62 (a, f, k), 5.76 (b, g, l), 5.9 (c, h, m), 6.06 (d, i, n), and 6.2 (e, j, o).

side surface of the cylinder there arise zones of positive velocity components corresponding to the upward and carrying flows and reaching 30–35% of the maximum velocity.

As mentioned above, the horizontal velocity component of the flow in all the indicated zones increases as the cylinder accelerates and its deflection from the vertical decreases, and the zones themselves turn together with the pendulum (the velocity reaches 0.65–0.7 before and 0.85 behind the body). At the same time, the velocity of the downward flows somewhat decreases (from 0.8 to 0.7), and it reaches the maximum at a larger distance from the body.

When the pendulum is at the lower point, in the narrow clearance between the cylinder and the cavity bottom there arises a carrying flow whose lines are somewhat shifted to the wall.

Analogously, the carrying flow above the cylinder propagates to the upper boundary of the square cavity, and the upward flow on the left of the body flows into the downward flow on the right of it. Consequently, the pendulum motion generates circulatory flow of the viscous fluid in the cavity; in this case, a zone of secondary vortex flow arises at the lower right corner.

Judging by the change in the vorticity fields near the moving cylinder, the near wake in the form of two vorticity plumes of different sign becomes more extended as the cylinder accelerates. Note that the vorticity field is asymmetric because the upper and lower halves of the body move with a different velocity. As a result, the vorticity generated in the neighborhood of the cylinder surface nearest to the center of the cavity is markedly smaller than the vorticity generated on the opposite side, which is more remote from the point of suspension. Nevertheless, the position of the stagnation point can be judged by the separation of the vorticity plumes generated on the front part of the cylinder. This point is positioned at the intersection of the mechanical trajectory with the front part of the cylinder contour. We are also interested in considering the zones of opposite-sign vorticity, which are induced in the neighborhood of the walls.

When the cylinder passes through the lower point of the trajectory, in the clearance between the cylinder and the cavity bottom there arises shear flow with two counterflows: carrying flow near the wall and flow of the viscous

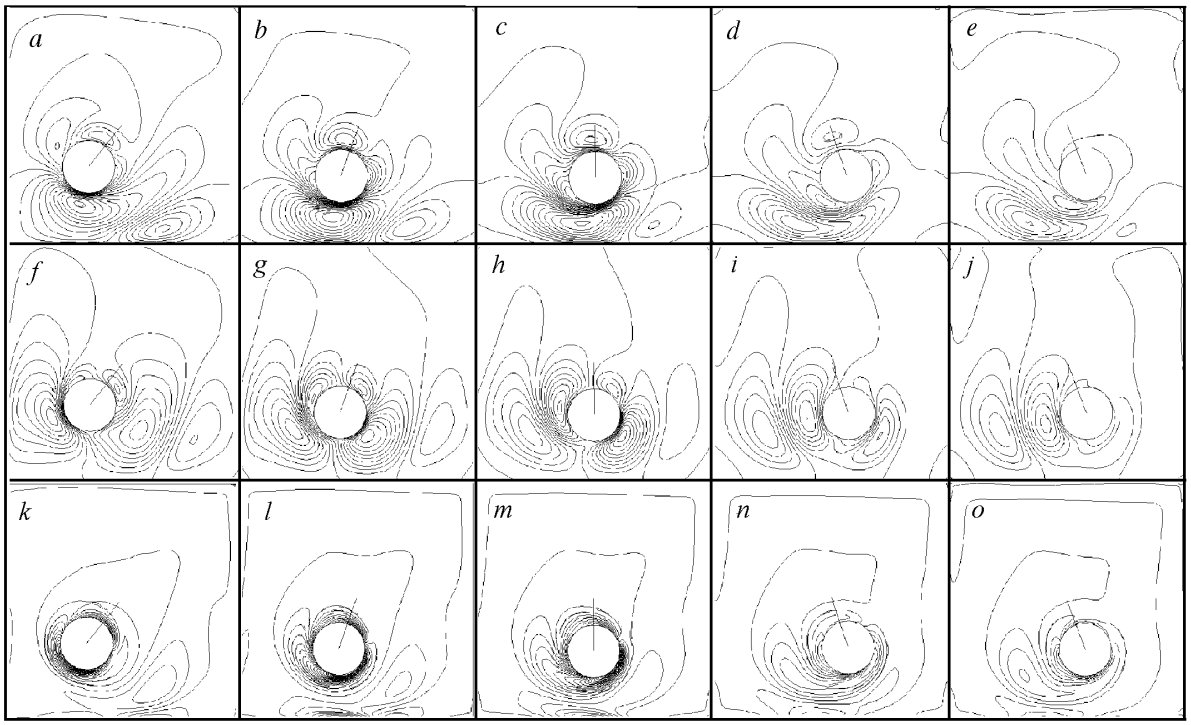

Fig. 8. Evolution of the patterns of flow around the circular cylinder in the second half-period of the pendular oscillations. The fields of isolines of the horizontal (a, b, c, d, e) and vertical (f, g, h, i, j) velocity components are drawn with a step of 0.05 and the fields of vorticity isolines (k, l, m, n, o) are drawn with a step of 0.5. The patterns were constructed at the instants of time t = 6.8 (a, f, k), 8 (b, g, l), 9.04 (c, h, m), 10.5 (d, i, n), and 11.2 (e, j, o).

fluid carried by the pendulum (Fig. 6). As the pendulum moves to the extreme left position, around it there gradually arises large-scale circulatory fluid motion extending over a significant part of the square cavity. In the wake behind the cylinder there arises a separated vortex that practically does not change its position and retains its intensity during the quarter of the oscillation period.

The evolution of the structure of the flow around the circular cylinder at its near-extreme left position is analyzed in Fig. 7. Over a comparatively long period of time (from t = 5.62 to t = 6.2) the body remains stationary and the flow field surrounding it experiences changes. The interaction of the flow induced by the pendulum motion with the pendulum itself has characteristic features. It should be noted first of all that the longitudinal velocity of the flow in the space above the cylinder somewhat decreases (approximately by 0.05) and the vertical velocity of the downward flow increases (by the same 0.05) to t = 6.06. Hereinafter, the velocity of the downward flow somewhat decreases. In this case, the positive longitudinal and transverse velocity components in the layer adjacent to the cylinder wall, which are due to the movement of the pendulum from the extreme position, increase. Judging by the vorticity field, the circular cylinder finds itself at the vorticity core, and with time the fluid in the near-wall layer turns over it. It should also be emphasized that by and large the structure of the vortex flow in the cavity does not change over the period of time under consideration. This is true first of all for the large-scale vortex at the lower right corner.

The final phase of the first oscillation period is illustrated in Fig. 8. The circular cylinder moves from the left to the right position in the disturbed field. The inertia of the flow formed in the cavity maintains the rotary motion (clockwise) of the fluid in the cavity. Therefore, the pendulum moves to meet the incoming flow. The most important feature of the considered phase of the oscillation process is the interaction of the circular cylinder with the large-scale vortex. The vortex becomes weaker as the lower point of the trajectory is approached and practically disappears after the passage through this point. It is also interesting to note that as the body moves to the central part of the cavity, the zone of the downward flow gradually disappears, i.e., the flow circulating clockwise becomes virtually blocked. The counterflow in the near-bottom part is displaced to the wall as the pendulum moves and the flow of the fluid car-

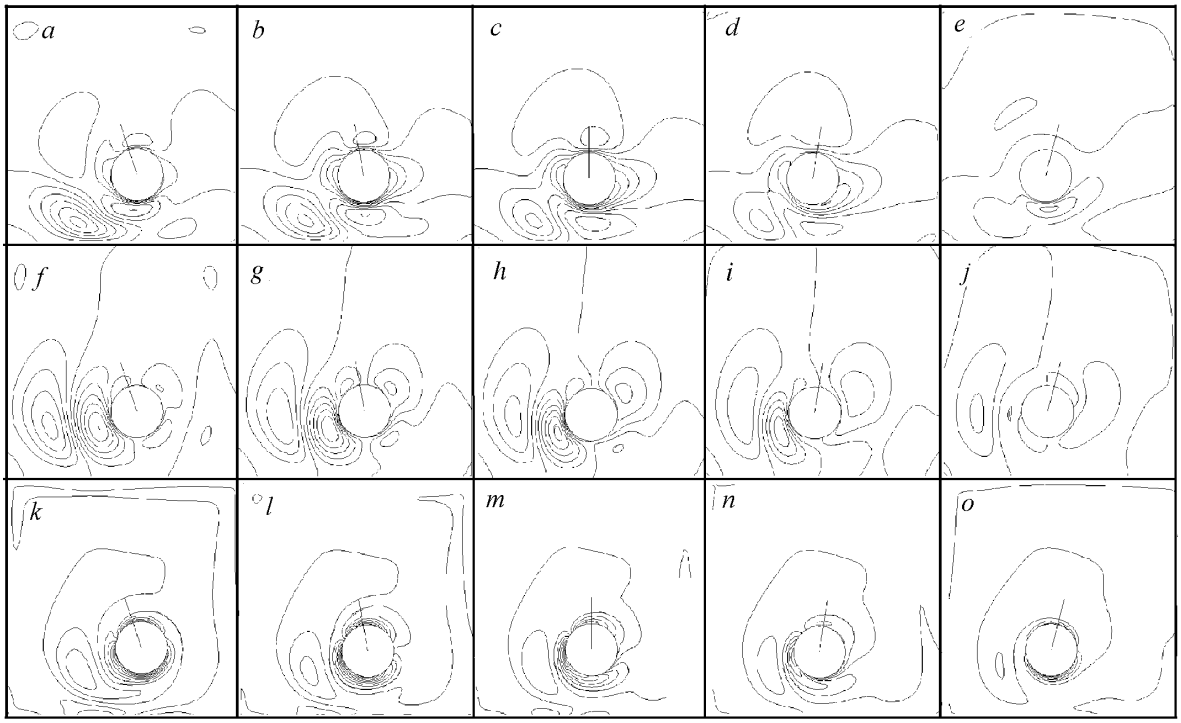

Fig. 9. Evolution of the patterns of flow around the circular cylinder in the third half-period of the pendular oscillations. The fields of isolines of the horizontal (a, b, c, d, e) and vertical (f, g, h, i, j) velocity components are drawn with a step of 0.5 and the fields of vorticity isolines (k, l, m, n, o) are drawn with a step of 0.5. The patterns were constructed at the instants of time t = 12 (a, f, k), 13 (b, g, l), 13.98 (c, h, m), 15 (d, i, n), and 16.52 (e, j, o).

ried by it intensifies. The upward flow near the left wall of the cavity flows into the downward flow not in the right part relative to the cylinder but in the neighborhood of the middle cross section. As a result, behind the circular cylinder moving to the right there arises a large-scale vortex swirling clockwise. It is interesting to follow the fluid motion near the right wall in the immediate vicinity of the body. The upward flow near the wall flows into the downward flow at a certain distance from the bottom. Thus, in the right part of the cavity there arises a reverse flow that is much weaker than the reverse flow in the left part.

Judging by the evolution of the vorticity fields, as in the first half-period of the oscillations, behind the moving body there arises a near wake in the form of two plumes with a different intensity and high vorticity. As the pendulum approaches the extreme right position, the vortex sheet separates and swirls into a large-scale vortex in the left half of the square cavity. Its intensity is practically equal to the intensity of the vortex occurring in the right part of the cavity a half-period before.

The next half-period of the oscillations is analyzed in Fig. 9. The movement of the body from the extreme right to the extreme left position is accompanied by the above-mentioned processes. However, the intensity of the flow is much smaller than that a half-period before. The interaction of the circular cylinder with the large-scale vortex substantially weakens it. However, the vortex exists even at the extreme left position of the pendulum, whereas a marked vortex is not formed on its right side.

CONCLUSION

Within the limits of the conjugate two-dimensional problem on oscillations of a circular cylinder in a square cavity filled with an incompressible viscous fluid we have performed a detailed analysis of the damping of pendular oscillations in the case where aluminum was used for the pendulum material and oil for the working medium. The extremum values of the flow parameters have been explained to a large measure on the basis of the analysis of the in-

terrelation between the vortex dynamics and the cyclic time changes in the integral and local hydrodynamic characteristics of the flow with allowance for the walls bounding the region of oscillations. The multiblock computational algorithm developed is based on the use of sliding structurized grids and allows one to calculate the movement of self-propelled objects in the air atmosphere.

This work was carried out with financial support from the Russian Foundation for Basic Research (projects 02-01-00670, 02-02-81035, and 02-01-01160).

NOTATION

t, time, sec; x, y, z, Cartesian coordinates; D, diameter of the cylinder, m; g, free-fall acceleration, m/sec^2; m, mass of the pendulum, kg; m_f, mass of the expelled fluid, kg; R, distance from the center of rotation to the center of mass of the body, m; J, moment of inertia, kg·m^2; ω, angular velocity, 1/sec; M_a, moment of aerodynamic forces, kg·m^2/sec^2; φ, deflections of the pendulum from the horizontal, deg; α, deflections of the pendulum from the vertical, deg; L, characteristic linear dimension, m; S, characteristic area, m^2; Ω, characteristic volume, m^3; V, characteristic velocity, m/sec; μ, coefficient of dynamic fluid viscosity, kg/(m·sec); ρ_f and ρ_b, densities of the fluid and the pendulum material respectively, kg/m^3; U, maximum rate of pendulum motion in a nonviscous medium; m_a, coefficient of aerodynamic moment; d/dt, total time derivative; u and v, horizontal and vertical velocity components; T, oscillation period, fractions of L/V; δt, time of stay of the pendulum at the extreme positions; X and Y, horizontal and vertical components of the aerodynamic force; Nt, Re, and Fr, Newton, Reynolds, and Froude numbers (Nt = ρ_b/ρ_f, Re = $\rho UD/\mu$, and Fr = $U/\sqrt{gD}$); a_p, coefficient of the diagonal term in the initial algebraic equation; E, E factor. Subscripts: parameters with a bar, dimensionless quantities; b, parameters of the body; f, parameters of the fluid; p, point; max and min, maximum and minimum values; a, aerodynamic; ext, extremum.

REFERENCES

1. S. É. Khaikin, *Physical Principles of Mechanics* [in Russian], Moscow (1971).
2. P. A. Baranov, S. A. Isaev, Yu. S. Prigorodov, et al., *Izv. Vyssh. Uchebn. Zaved., Aviats. Tekh.*, No. 3, 30–35 (1999).
3. P. A. Baranov, S. A. Isaev, Yu. S. Prigorodov, et al., *Pis'ma Zh. Tekh. Fiz.*, **24**, Issue 8, 33–41 (1998).
4. S. A. Isaev, Yu. S. Prigorodov, and A. G. Sudakov, *Izv. Ross. Akad. Nauk, Mekh. Zhidk. Gaza*, No. 4, 88–96 (2000).
5. P. A. Baranov, S. A. Isaev, and A. G. Sudakov, *Izv. Ross. Akad. Nauk, Mekh. Zhidk. Gaza*, No. 2, 68–74 (2000).
6. P. A. Baranov, S. A. Isaev, and A. E. Usachov, *Inzh.-Fiz. Zh.*, **73**, No. 3, 606–613 (2000).
7. S. A. Isaev, A. G. Sudakov, P. A. Baranov, et al., *Inzh.-Fiz. Zh.*, **75**, No. 2, 28–35 (2002).
8. S. A. Isaev, V. L. Zhdanov, P. A. Baranov, et al., *Numerical Modeling of Laminar and Turbulent Flows past a Circular Cylinder with Inner Passages and Windows in the Contour* [in Russian], Preprint No. 3 of the A. V. Luikov Heat and Mass Transfer Institute, Minsk (2002).
9. S. A. Isaev, A. G. Sudakov, A. E. Usachov, et al., *Inzh.-Fiz. Zh.*, **75**, No. 5, 41–48 (2002).
10. S. A. Isaev, in: *Proc. Int. Conf. on Methods of Aerophysical Research*, Pt. 1, Novosibirsk (2002), pp. 102–107.
11. P. A. Baranov, S. V. Guvernyuk, M. A. Zubin, et al., *Izv. Ross. Akad. Nauk, Mekh. Zhidk. Gaza*, No. 2, 44–56 (2000).
12. A. E. Usachov, A. G. Sudakov, and V. L. Zhdanov, in: *Proc. 2nd East Europ. Conf. on Wind Eng.*, Vol. 1, 7–11 September 1998, Prague (1998), pp. 143–148.
13. W. Jia and Y. Nakamura, *JSME Int. J., Ser. B*, **39**, No. 2, 315–325 (1996).
14. I. A. Belov, S. A. Isaev, and V. A. Korobkov, *Problems and Methods for Calculation of Separated Flows of an Incompressible Fluid* [in Russian], Leningrad (1989).
15. J. H. Ferziger and M. Peric, *Computational Methods for Fluid Dynamics*, Springer, Berlin (1999).
16. S. M. Belotserkovskii and M. I. Nisht, *Separated and Unseparated Liquid Flows past Thin Wings* [in Russian], Moscow (1978).